

## Isotope Effects and the Nature of Selectivity in Rhodium-Catalyzed Cyclopropanations

Daniel T. Nowlan III,<sup>†</sup> Timothy M. Gregg,<sup>‡</sup> Huw M. L. Davies,<sup>\*‡</sup> and Daniel A. Singleton<sup>\*‡</sup>

Contribution from the Department of Chemistry, Texas A&M University, P.O. Box 30012, College Station, Texas 77842, and Department of Chemistry, State University of New York at Buffalo, Buffalo, New York 14260

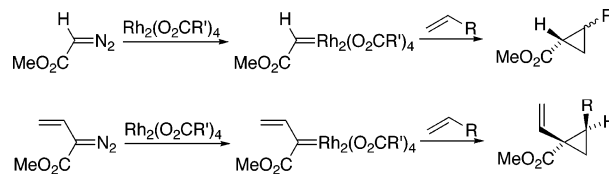
Received May 8, 2003; E-mail: singleton@mail.chem.tamu.edu; hdavies@acsu.buffalo.edu.

**Abstract:** The mechanism of the dirhodium tetracarboxylate catalyzed cyclopropanation of alkenes with both unsubstituted diazoacetates and vinyl- and phenyldiazoacetates was studied by a combination of <sup>13</sup>C kinetic isotope effects and density functional theory calculations. The cyclopropanation of styrene with methyl phenyldiazoacetate catalyzed by Rh<sub>2</sub>(octanoate)<sub>4</sub> exhibits a substantial <sup>13</sup>C isotope effect (1.024) at the terminal olefinic carbon and a smaller isotope effect (1.003–1.004) at the internal olefinic carbon. This is consistent with a highly asynchronous cyclopropanation process. Very similar isotope effects were observed in a bisrhodium tetrakis[(S)-N-(dodecylbenzenesulfonyl)prolinate] (Rh<sub>2</sub>(S-DOSP)<sub>4</sub>) catalyzed reaction, suggesting that the chiral catalyst engages in a very similar cyclopropanation transition-state geometry. Cyclopropanation with ethyl diazoacetate was concluded to involve an earlier transition state, based on a smaller terminal olefinic isotope effect (1.012–1.015). Density functional theory calculations (B3LYP) predict a reaction pathway involving complexation of the diazoesters to rhodium, loss of N<sub>2</sub> to afford a rhodium carbenoid, and an asynchronous but concerted cyclopropanation transition state. The isotope effects predicted for reaction of a phenyl-substituted rhodium carbenoid with styrene match within the error of the experimental values, supporting the accuracy of the theoretical calculations and the rhodium carbenoid mechanism. The accuracy of the calculations is additionally supported by excellent predictions of reaction barriers, stereoselectivity, and reactivity trends. The nature of alkene selectivity and diastereoselectivity effects in these reactions is discussed, and a new model for enantioselectivity in Rh<sub>2</sub>(S-DOSP)<sub>4</sub>-catalyzed cyclopropanations is presented.

### Introduction

The rhodium-catalyzed cyclopropanation of alkenes with  $\alpha$ -diazocarbonyls is a powerful method for the synthesis of functionalized cyclopropanes. Most such cyclopropanations have been carried out using simple  $\alpha$ -diazocarbonyls such as diazoacetates, but a common problem in these reactions is low selectivity.<sup>1</sup> The presumed intermediate rhodium carbenoids derived from diazoacetates are highly reactive and electrophilic, and we will describe them as “unstabilized carbenoids”. Except for very bulky analogues, unstabilized carbenoids exhibit low diastereoselectivity.<sup>2</sup> They also show low substrate selectivity and are prone to dimerization.<sup>3</sup> The development of cyclopropanations with diazoacetates that are both highly enantioselective and highly diastereoselective has proven to be a particular challenge,<sup>4</sup> outside of intramolecular reactions.<sup>5</sup>

Because of this problem, there has been considerable interest in the greater stereoselectivity and chemoselectivity exhibited



in reactions involving vinyl-, aryl-, and alkynyldiazoacetates.<sup>6</sup> The “stabilized carbenoids” derived from these substrates generally afford high diastereoselectivity in cyclopropanations. Fewer side reactions are observed; dimerization products, for example, are very rarely observed. The stabilized carbenoids

<sup>†</sup> Texas A&M University.

<sup>‡</sup> State University of New York at Buffalo.

- (1) Doyle, M. P.; Griffin, J. H.; Bagheri, V.; Dorow, R. L. *Organometallics* **1984**, *3*, 53–61.
- (2) Doyle, M. P.; Bagheri, V.; Wandless, T. J.; Harn, N. K.; Brinker, D. A.; Eagle, C. T.; Loh, K.-L. *J. Am. Chem. Soc.* **1990**, *112*, 1906–1912.
- (3) Davies, H. M. L.; Hodges, L. M.; Matasi, J. J.; Hansen, T.; Stafford, D. G. *Tetrahedron Lett.* **1998**, *39*, 4417–4420.

- (4) The only effective catalysts for highly enantioselective and diastereoselective cyclopropanations with ethyl diazoacetate have been ruthenium-based catalysts. For examples, see: (a) Nishiyama, H.; Itoh, Y.; Matsumoto, H.; Park, S.-B.; Itoh, K. *J. Am. Chem. Soc.* **1994**, *116*, 2223–2224. (b) Frauenkron, M.; Berkessel, A. *Tetrahedron Lett.* **1997**, *38*, 7175–7176. (c) Bachmann, S.; Furler, M.; Mezzetti, A. *Organometallics* **2001**, *20*, 2102–2108. (d) Werle, T.; Maas, G. *Adv. Synth. Catal.* **2001**, *343*, 37–40.
- (5) Doyle, M. P.; Austin, R. E.; Bailey, A. S.; Dwyer, M. P.; Dyatkin, A. B.; Kalinin, A. V.; Kwan, M. M. Y.; Liras, S.; Oalman, C. J.; Pieters, R. J.; Protopopova, M. N.; Raab, C. E.; Roos, G. H. P.; Zhou, Q.-L.; Martin, S. F. *J. Am. Chem. Soc.* **1995**, *117*, 5763–5775. (b) Doyle, M. P.; Zhou, Q.-L.; Dyatkin, A. B.; Ruppert, D. A. *Tetrahedron Lett.* **1995**, *36*, 7579–7582.
- (6) (a) Davies, H. M. L.; Clark, T. J.; Church, L. A. *Tetrahedron Lett.* **1989**, *30*, 5057–5060. (b) Davies, H. M. L.; Bruzinski, P. R.; Fall, M. J. *Tetrahedron Lett.* **1996**, *37*, 4133–4136. (c) Davies, H. M. L.; Boebel, T. A. *Tetrahedron Lett.* **2000**, *41*, 8189–8192.

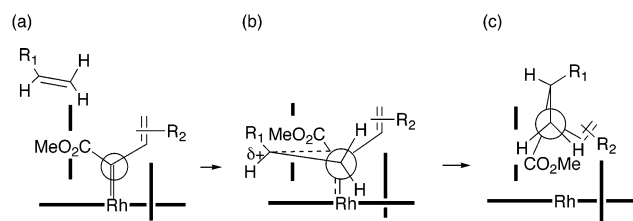
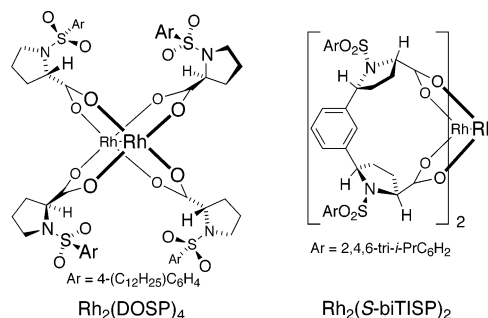


**Figure 1.** (a) Alkene approach at the top face of the carbenoid from a sideways trajectory (least encumbered approach). (b) “Side-on” transition state for cyclopropanation. (c) Cyclopropane formed with absolute stereochemistry set.

are still reactive but behave as if they are much more sterically demanding than the traditional carbenoids. Intermolecular cyclopropanation of monosubstituted, 1,1-disubstituted, and *cis*-1,2-disubstituted alkenes is very favorable, but *trans*-1,2-disubstituted alkenes cannot be cyclopropanated by this class of carbenoids.<sup>7</sup> This reactivity profile is very different from that of the carbenoid derived from ethyl diazoacetate, which is capable of cyclopropanation of even tetrasubstituted alkenes.<sup>1</sup> The stabilized carbenoids exhibit much greater kinetic selectivity between alkenes and high regioselectivity in reactions with 1,3-dienes. Cyclopropanations with vinyl diazoacetates have proven particularly useful in the stereoselective synthesis of functionalized five- and seven-membered rings.<sup>8</sup>

A highly advantageous characteristic of stabilized carbenoids is that they undergo highly enantioselective cyclopropanations when dirhodium tetraprolineates, such as bisrhodium tetrakis[(*S*)-*N*-(dodecylbenzenesulfonyl)proline] ( $\text{Rh}_2(\text{S-DOSP})_4$ )<sup>7,9</sup> and bisrhodium bis[(*5S,5'S*)-5,5'-(1,3-phenylene)bis[*N*-(2,4,6-triisopropylbenzenesulfonyl)-*L*-proline]] ( $\text{Rh}(\text{S-biTISP})_2$ ),<sup>10</sup> are used as catalysts. A useful predictive model for the stereochemical outcome of these cyclopropanations has been developed and is outlined in Figure 1.<sup>7</sup> In this model the cyclopropanation is considered to be concerted but asynchronous, and the alkene approaches the carbenoid with a “side-on” trajectory preferentially over the ester group. The dirhodium tetraprolineate catalysts are considered to adopt a  $D_2$  symmetric arrangement. For  $\text{Rh}_2(\text{S-DOSP})_4$ , it is assumed that the  $D_2$  symmetric arrangement is the preferred solution-phase conformation,<sup>7</sup> while the bridging ligands in  $\text{Rh}_2(\text{S-biTISP})_2$  lock this complex in a  $D_2$  symmetric arrangement.<sup>10</sup> Due to the high symmetry of the catalysts, they can be simply viewed as a catalyst wall with two blocking groups, one in the front and one in the back of the catalyst. This model comfortably explains why *trans* alkenes are particularly unreactive, along with the ultimate *cis* orientation of the vinyl (or aryl) group and the alkene substituent in the product cyclopropane. The side-on approach also predicts the absolute stereochemistry observed in these cyclopropanations.<sup>7</sup>

Even though this model has been a reliable predictive tool for the cyclopropanation stereochemistry, as the chemistry has evolved, certain inconsistencies have become apparent. For example,  $\text{Rh}_2(\text{S-DOSP})_4$  and  $\text{Rh}_2(\text{S-biTISP})_2$  actually give

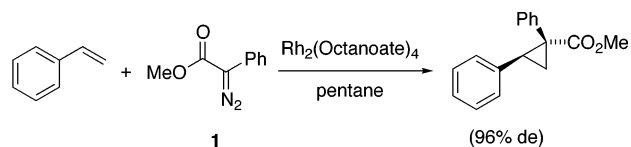


opposite asymmetric induction in the cyclopropanation chemistry, although this effect can be rationalized by assuming that the carbenoids bind in a different staggered conformation in these catalysts.<sup>10</sup> A more perplexing result is the highly enantioselective 3 + 2 cycloaddition between vinylcarbenoids and certain vinyl ethers,<sup>11</sup> which appears to be a concerted process that would require the vinyl ether to approach over the vinyl group, yet the absolute stereochemistry is opposite to that predicted by such an approach of the vinyl ether. A further concern is the lack of a good rationalization why the side-on approach over the ester group should be so strongly preferred compared to the approach over the electron-donating group.

Any such qualitative model built on experimental observations may be supplanted as more physical information becomes available, and a physically accurate model is likely to perform superiorly in the understanding and prediction of new chemistry. We therefore sought to define an accurate trajectory of approach of the alkene to the carbenoid. We describe here a combined experimental and theoretical study of the rhodium-catalyzed cyclopropanation of alkenes with both simple diazoacetates and vinyl- and aryldiazoacetates. The results delineate the mechanistic differences between cyclopropanations with unstabilized versus stabilized carbenoids, providing a clear picture of the factors influencing selectivity in these reactions. Finally, the experimentally supported transition-state geometries, in which the alkene approaches the carbenoid in an “end-on” rather than a side-on fashion, lead to new explanations for both diastereoselectivity and enantioselectivity in these reactions.

## Results and Discussion

**Experimental Isotope Effects.** As a typical example of an intermolecular cyclopropanation with an aryldiazoacetate, the cyclopropanation of styrene with methyl phenyldiazoacetate (**1**) catalyzed by  $\text{Rh}_2(\text{octanoate})_4$  was chosen for study. This reaction is highly diastereoselective and affords the cyclopropanation product cleanly without observable side reactions of the styrene. The <sup>13</sup>C kinetic isotope effects (KIEs) for this reaction were measured at natural abundance by NMR methodology.<sup>12</sup>



A challenge was to carry out the reaction under the constraints necessary for the measurement of KIEs, including the require-

(11) Davies, H. M. L.; Xiang, B.; Kong, N.; Stafford, D. G. *J. Am. Chem. Soc.* **2001**, *123*, 7461–7462.

(12) Singleton, D. A.; Thomas, A. A. *J. Am. Chem. Soc.* **1995**, *117*, 9357–9358.

(7) Davies, H. M. L.; Bruzinski, P. R.; Lake, D. H.; Kong, N.; Fall, M. J. *J. Am. Chem. Soc.* **1996**, *118*, 6897–6907.

(8) (a) Davies, H. M. L.; Hu, B. *J. Org. Chem.* **1992**, *57*, 4309–4312. (b) Davies, H. M. L.; Hu, B. *J. Org. Chem.* **1992**, *57*, 3186–3190. (c) Davies, H. M. L.; Clark, T. J.; Smith, H. D. *J. Org. Chem.* **1991**, *56*, 3817–3824. (d) Davies, H. M. L.; Stafford, D. G.; Doan, B. D.; Houser, J. H. *J. Am. Chem. Soc.* **1998**, *120*, 3326–3331.

(9) (a) Davies, H. M. L.; Hutcheson, D. K. *Tetrahedron Lett.* **1993**, *34*, 7243–7246. (b) Davies, H. M. L.; Townsend, R. J. *J. Org. Chem.* **2001**, *66*, 6595–6603.

(10) Davies, H. M. L.; Panaro, S. A. *Tetrahedron Lett.* **1999**, *40*, 5287–5290.

ments that all of the styrene be present at the beginning of the reaction and that the styrene be taken to high conversion. This was accomplished by adding **1** slowly, by syringe pump, to a solution of styrene and 0.1 mol %  $\text{Rh}_2(\text{octanoate})_4$  in dry pentane. Reactions on an  $\approx 100$  mmol scale at 25 °C were taken to 84 and 83% conversion (based on the remaining styrene determined by NMR,  $\approx \pm 1\%$ ), and the unreacted styrene was recovered by chromatography followed by distillation. The recovered material was analyzed by  $^{13}\text{C}$  NMR along with a standard sample of the styrene not subjected to the reaction conditions. The changes in isotopic composition were determined relative to the para carbon, assuming that its isotopic composition does not change. From the changes in isotopic composition, the  $^{13}\text{C}$  isotope effects were calculated as previously described.<sup>12</sup>

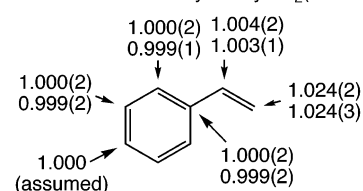
The comparison reaction of styrene with ethyl diazoacetate was studied similarly, with the presumably minor differences that the reaction employed 0.04 mol %  $\text{Rh}_2(\text{OAc})_4$  as catalyst and was carried out in dichloromethane. The ethyl diazoacetate reaction is much less diastereoselective than that of **1**, affording a 1.5:1 mixture of trans and cis cyclopropanation products as previously reported.<sup>13</sup> Three reactions on a 130 mmol scale at 25 °C were taken to 80, 81, and 88% conversion, and the unreacted styrene was recovered and analyzed as above to determine the  $^{13}\text{C}$  isotope effects.

A final isotope effect determination was performed to compare the reaction with **1** catalyzed by  $\text{Rh}_2(\text{octanoate})_4$  with an asymmetric cyclopropanation catalyzed by  $\text{Rh}_2(\text{S-DOSP})_4$ . The  $\text{Rh}_2(\text{S-DOSP})_4$ -catalyzed reaction proceeds in 91% ee and 94% de.<sup>14</sup> The  $^{13}\text{C}$  KIEs in this case were determined from analysis of styrene recovered from a reaction taken to 84% conversion at 0 °C.

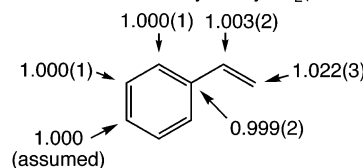
The resulting isotope effects are summarized in Figure 2. The  $\text{Rh}_2(\text{octanoate})_4$ -catalyzed cyclopropanation with **1** exhibits a substantial  $^{13}\text{C}$  KIE at the terminal olefinic carbon, a smaller but consistently significant KIE at the internal olefinic carbon and small or negligible KIEs at the aromatic ring carbons. The large isotope effect at the terminal olefinic carbon qualitatively suggests substantial bond formation to this carbon in the rate-limiting step. In combination with the much smaller isotope effect at the internal olefinic carbon, the results suggest a highly asynchronous cyclopropanation transition state. In fact, the KIEs by themselves would not qualitatively exclude a stepwise process,<sup>15</sup> but this seems unlikely given the general stereospecificity of rhodium-catalyzed cyclopropanations. A quantitative interpretation of the KIEs will be given below. The isotope effects observed for the  $\text{Rh}_2(\text{S-DOSP})_4$ -catalyzed reaction are within experimental error of the  $\text{Rh}_2(\text{octanoate})_4$ -catalyzed results. This suggests that the use of the bulky chiral catalyst does not greatly affect the geometry of the cyclopropanation transition state.

The most notable difference in the cyclopropanation with ethyl diazoacetate is that the terminal olefinic KIE is much smaller. Since the reactions of both **1** and ethyl diazoacetate

Reaction with **1** catalyzed by  $\text{Rh}_2(\text{Octanoate})_4$



Reaction with **1** catalyzed by  $\text{Rh}_2(\text{S-DOSP})_4$



Reaction with ethyl diazoacetate

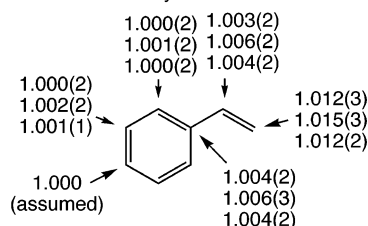


**Figure 2.**  $^{13}\text{C}$  KIEs ( $k^{12}\text{C}/k^{13}\text{C}$ ) for the reaction of styrene with **1** or ethyl diazoacetate. Standard deviations ( $n = 6$ ) in the last digit are shown in parentheses.

are highly exothermic, so that both should have a relatively early transition state, the  $^{13}\text{C}$  KIEs would be qualitatively interpreted as implying a significantly earlier transition state with ethyl diazoacetate than with **1**.

**Theoretical Calculations.** The pathway for reaction of models methyl diazoacetate (**2**) and methyl vinyldiazoacetate (**3**) with styrene catalyzed by model  $\text{Rh}_2(\text{O}_2\text{CH})_4$ <sup>16</sup> was studied in B3LYP calculations employing a LANL2DZ basis set and effective core potential on rhodium and a 6-31G\* basis set on the remaining atoms.<sup>17</sup> Previous work has supported the ability of these calculations to adequately predict ground-state structures and reasonable mechanistic pathways for reactions of dirhodium tetracarboxylate complexes.<sup>18,19,20</sup> The accuracy of these calculations for transition structures in rhodium-mediated cyclo-

(13) Anciaux, A. J.; Hubert, A. J.; Noels, A. F.; Petinot, N.; Teyssié, P. J. *Org. Chem.* **1980**, *45*, 695–702.

(14) Davies, H. M. L.; Rusiniak, L. *Tetrahedron Lett.* **1998**, *39*, 8811–8812.

(15) The  $^{13}\text{C}$  KIEs observed here are consistent with those observed in asynchronous but concerted Diels–Alder reactions. See: (a) Singleton, D. A.; Merrigan, S. R.; Beno, B. R.; Houk, K. N. *Tetrahedron Lett.* **1999**, *40*, 5817–21. (b) Singleton, D. A.; Schulmeier, B. E.; Hang, C.; Thomas, A. A.; Leung, S.-W.; Merrigan, S. R. *Tetrahedron* **2001**, *57*, 5149–5160.

(16) The minimal  $\text{Rh}_2(\text{O}_2\text{CH})_4$  was judged to be a sufficient model for  $\text{Rh}_2(\text{octanoate})_4$  based on similar geometries for transition structure **13** versus the corresponding transition structure with  $\text{Rh}_2(\text{OAc})_4$  (see Supporting Information; differences of 0.018, 0.006, 0.042, and 0.028 Å were predicted for the Rh–Rh, Rh–C, and the two incipient C–C bonding distances, respectively). Although the experimental reactions could have been carried out using  $\text{Rh}_2(\text{O}_2\text{CH})_4$ , the low solubility of  $\text{Rh}_2(\text{O}_2\text{CH})_4$  would have increased concerns over the identity of the actual catalyst.

(17) Frisch, M. J.; Trucks, G. W.; Schlegel, H. B.; Scuseria, G. E.; Robb, M. A.; Cheeseman, J. R.; Zakrzewski, V. G.; Montgomery, J. A., Jr.; Stratmann, R. E.; Burant, J. C.; Dapprich, S.; Millam, J. M.; Daniels, A. D.; Kudin, K. N.; Strain, M. C.; Farkas, O.; Tomasi, J.; Barone, V.; Cossi, M.; Cammi, R.; Mennucci, B.; Pomelli, C.; Adamo, C.; Clifford, S.; Ochterski, J.; Petersson, G. A.; Ayala, P. Y.; Cui, Q.; Morokuma, K.; Malick, D. K.; Rabuck, A. D.; Raghavachari, K.; Foresman, J. B.; Cioslowski, J.; Ortiz, J. V.; Stefanov, B. B.; Liu, G.; Liashenko, A.; Piskorz, P.; Komaromi, I.; Gomperts, R.; Martin, R. L.; Fox, D. J.; Keith, T.; Al-Laham, M. A.; Peng, C. Y.; Nanayakkara, A.; Gonzalez, C.; Challacombe, M.; Gill, P. M. W.; Johnson, B. G.; Chen, W.; Wong, M. W.; Andres, J. L.; Head-Gordon, M.; Replogle, E. S.; Pople, J. A. *Gaussian 98*, Revision A.11.2; Gaussian, Inc.: Pittsburgh, PA, 2001.

(18) (a) Sheehan, S. M.; Padwa, A.; Snyder, J. P. *Tetrahedron Lett.* **1998**, *39*, 949–952. (b) Padwa, A.; Snyder, J. P.; Curtis, E. A.; Sheehan, S. M.; Worsencroft, K. J.; Kappe, C. O. *J. Am. Chem. Soc.* **2000**, *122*, 8155–8167.

(19) Nakamura, E.; Yoshikai, N.; Yamanaka, M. *J. Am. Chem. Soc.* **2002**, *124*, 7181–7192.

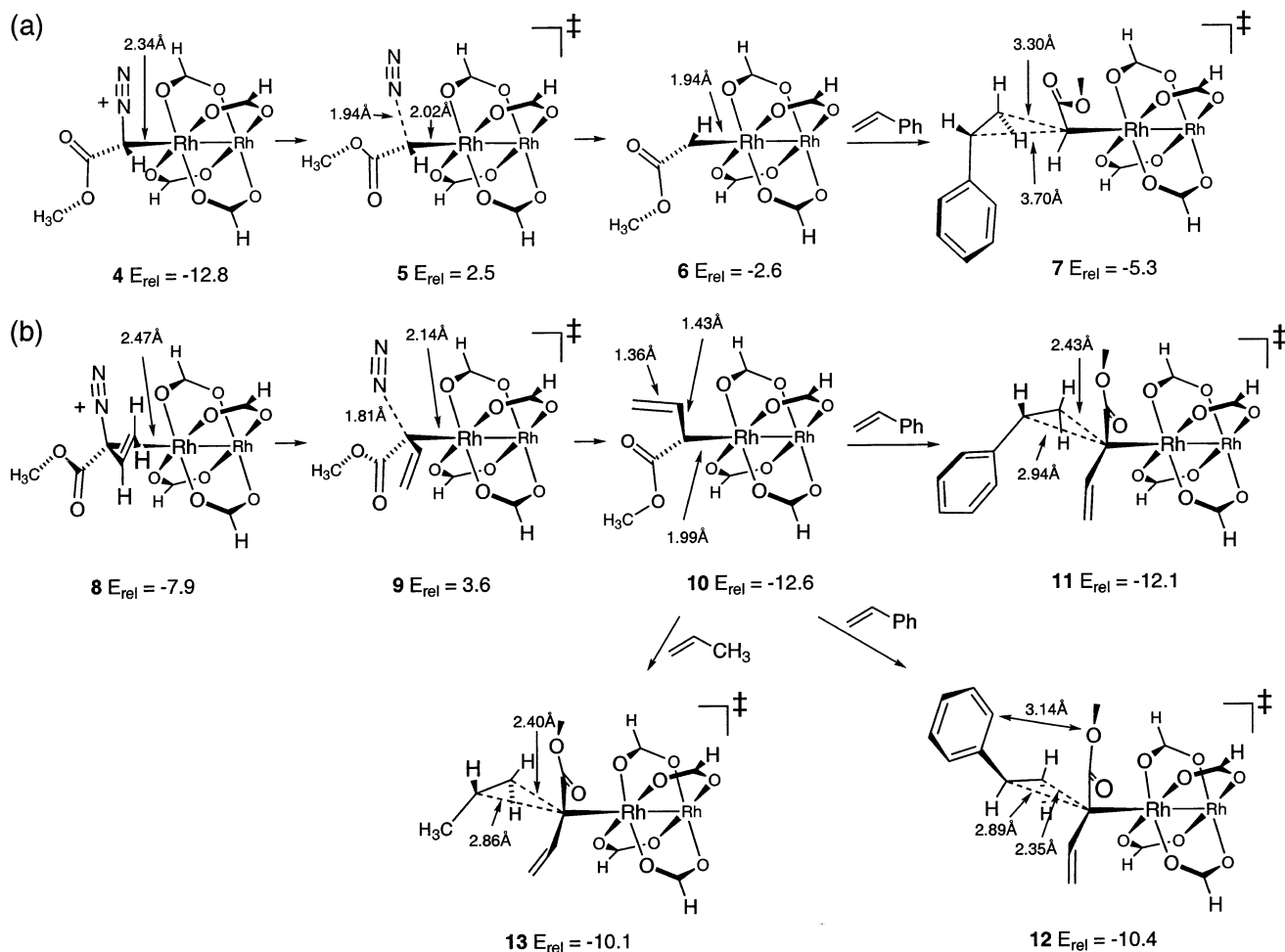


**Figure 3.** (a) Calculated pathway for cyclopropanation of styrene with methyl diazoacetate ( $\text{HCN}_2\text{CO}_2\text{CH}_3$ , **2**) catalyzed by model  $\text{Rh}_2(\text{O}_2\text{CH})_4$ . (b) Calculated pathway for cyclopropanation of styrene or propene with methyl vinyl diazoacetate ( $\text{H}_2\text{C}=\text{CHCN}_2\text{CO}_2\text{CH}_3$ , **3**) catalyzed by model  $\text{Rh}_2(\text{O}_2\text{CH})_4$ . Relative energies (B3LYP + zpe) compared to starting materials are given in kilocalories per mole.

propanations will be gauged here by comparison of predicted and experimental isotope effects. The only pathway studied in detail for these reactions was the Yates mechanism involving complexation of the diazoesters to rhodium, loss of  $\text{N}_2$  to afford a rhodium carbenoid, and cyclopropanation by the rhodium carbenoid.<sup>21</sup> An alternative mechanism involving direct reaction of styrene with a diazoester-rhodium complex was explored briefly, but no transition structure corresponding to this process could be located.

No allowance was made for solvent effects in these calculations—all of the intermediate complexes exhibit some charge separation, with predicted dipole moments of 4–8 D, compared to less polar starting materials. Thus, the general expectation is that the calculations will underestimate the stability of the intermediate complexes. When calculated energies are compared to the actual solution chemistry, an additional consideration is that the starting rhodium tetracarboxylate would likely be ligated by *some* ligand in the absence of special precautions.<sup>22</sup> This makes it particularly difficult to estimate

the entropy of complexation of diazoesters to the starting rhodium complex.

The overall pathways predicted for these reactions are shown in Figure 3. Multiple rotamers were explored for each intermediate or transition structure on each pathway, and a total of two distinct conformers were located for **2**, **4**, **5**, **7**, **8**, and **10**, three for **9** and **12**, four for **3** and **11**, and seven for **13**. The lowest energy structures are depicted schematically in Figure 3. Stereoviews for all structures are given in the Supporting Information.

The initial complexation of **2** and **3** with  $\text{Rh}_2(\text{O}_2\text{CH})_4$  to afford **4** and **8**, respectively, is predicted to be exothermic in both cases. Loss of  $\text{N}_2$  from **4** via transition structure **5** then faces a predicted barrier of 15.3 kcal/mol. This would be the turnover-limiting barrier for the catalytic cycle, and the predicted barrier is in excellent agreement with the  $\Delta H^\ddagger = 15.1$  kcal/mol found by Hubert and Noels for the  $\text{Rh}_2(\text{OAc})_4$ -catalyzed cyclopropanation of styrene with ethyl diazoacetate.<sup>13</sup> The predicted barrier may also be compared with a recently reported experimental free-energy of activation of 13.3 kcal/mol for loss of  $\text{N}_2$  from a diazoketone.<sup>23</sup> The calculated energetics are thus consistent with Pirrung's observation of Michaelis–Menten kinetics in similar

(20) For a discussion of theoretical methods applied to transition-metal containing systems, see: Siegbahn, P. E. M.; Blomberg, M. R. A. *Chem. Rev.* **2000**, *100*, 421–437.

(21) Yates, P. J. *Am. Chem. Soc.* **1952**, *74*, 5376–5381.

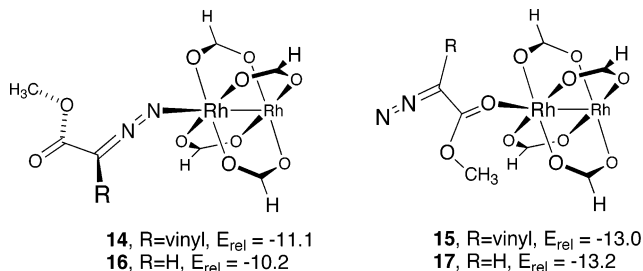
(22) Cotton, F. A.; Hilliard, E. A.; Murillo, C. A. *J. Am. Chem. Soc.* **2002**, *124*, 5658–5660.

(23) Pirrung, M. C.; Liu, H.; Morehead, A. T., Jr. *J. Am. Chem. Soc.* **2002**, *124*, 1014–1023.

reactions as well as his proposal that the resting saturated catalyst is a rhodium-diazocarbonyl complex.<sup>23</sup> Similar predicted energetics have recently been reported by Nakamura for the reaction of **2** with  $\text{Rh}_2(\text{O}_2\text{CH})_4$ .<sup>19</sup>

The complexation of  $\text{Rh}_2(\text{O}_2\text{CH})_4$  with **3** is predicted to be much weaker than with **2**. This might be expected on the basis of a greater loss of stabilizing conjugation on complexation, but the prediction was not initially reconcilable with some experimental observations. First, because of the higher energy of **8** compared with **4**, the turnover-limiting barrier for the catalytic cycle with **3** (11.6 kcal/mol) would be much less than with **2** (15.3 kcal/mol). Thus, the overall reaction of vinyl- or aryldiazoacetates would be expected to be much faster than with unsubstituted diazoacetates. This is not observed. In side-by-side reactions using **1** versus **3** with  $\text{Rh}_2(\text{octanoate})_4$  as catalyst in toluene at 0 °C, the two reactions exhibited very similar initial rates based on the evolution of  $\text{N}_2$  (see Supporting Information). A second experimental observation that did not fit with the high energy of **8** was Pirrung's report of a similar  $K_m$  for reactions of **1** compared to unsubstituted diazocarbonyls.<sup>23</sup> From the energy of model **8**, one would expect **1** to exhibit a  $K_m$  that is approximately 4 orders of magnitude higher than unsubstituted cases.

These observations suggested that some alternative complex, more stable than **8**, was present in reactions of vinyl- and aryldiazoacetates. We therefore explored the stability of complexes in which **2** or **3** is coordinated to  $\text{Rh}_2(\text{O}_2\text{CH})_4$  through either the carbonyl oxygen or the terminal nitrogen of the diazo group. All of the resulting complexes **14**–**17** were predicted to be lower in energy than **8**. For the unsubstituted complexes derived from **2**, the O-linked **17** and the C-linked **4** are predicted to be similar in energy and the calculation here would not resolve which is more stable in solution. For the vinyl-substituted complexes, the O-linked **15** is lower in energy than the N-linked **14** by 1.9 kcal/mol. However, **14** has a very low energy Rh–N rotational mode (11  $\text{cm}^{-1}$ ) that increases its entropy, so that **14** and **15** are within 0.1 kcal/mol when their free energies are estimated. Both **14** and **15** are comparable in energy to **4** and **17**. The overall reaction rate would be decided by the difference in energy between **14/15** and **9**, and the apparent  $K_m$  under such circumstances would reflect the energy of **14/15** despite their being bystanders to the reaction pathway. For the unsubstituted complexes, bystander **17** is similar in energy to **4** and so would have little effect on  $K_m$ . Overall, the reversible formation of complexes like **14** and **15** would result in catalytic rates and  $K_m$ 's that are similar for substituted versus unsubstituted diazocarbonyls. This fits well with the experimental observations above.



As predicted for a similar rhodium carbenoid,<sup>18b</sup> formation of the unsubstituted carbenoid **6** is only slightly downhill from

the starting materials. However, the vinylcarbenoid **10** is predicted to be substantially more stable. In both structures, the ester carbonyl is twisted out of conjugation and it appears positioned to align its  $\pi^*$  orbital with the electron-rich Rh–C bond (the Rh–C–C=O dihedral angle in **10** is 101.5°). This hyperconjugative interaction is evidently more favorable than having the carbonyl conjugated with the electron-deficient carbene center. In contrast the vinyl group in **10** is well-aligned to donate to the carbene. In fact, **10** has some structural characteristics resembling a  $\sigma$ -complex of an allylic cation with the rhodium. In a Mullikin analysis the vinylic group of **10** has a net charge of +0.23, compared to +0.40 in  $\text{H}_2\text{C}=\text{CH}-\text{C}^+(\text{OH})(\text{CO}_2\text{CH}_3)$  (B3LYP/6-31G\*). The allylic bond lengths of 1.36 and 1.43 Å in **10** are identical to those predicted for  $\text{H}_2\text{C}=\text{CH}-\text{C}^+(\text{OH})(\text{CO}_2\text{CH}_3)$ . One experimental observation that supports the greater stability of carbenes such as **10** is that reactions of vinyl- and aryldiazoacetates usually do not afford dimerization products.<sup>3</sup>

There was no predicted potential energy barrier for reaction of the unstabilized carbenoid **6** with styrene. Since B3LYP calculations tend to underestimate barriers, the energy surface was also explored in MPW1K calculations,<sup>24</sup> but still no potential energy saddle point could be located. The approximate variational transition state **7** was located iteratively as a maximum in the free energy (calculating entropy and enthalpic and zero-point energy (zpe) corrections from unscaled frequencies at 298 K). This process is subject to multiple interrelated problems, due to the difficulty of accurately calculating low frequencies and their associated entropy and the questionable accuracy of the predicted potential energy surface at long styrene–carbene distances. For this reason the detailed structure of **7** should not be overinterpreted. However, the calculations clearly predict that the reaction of **6** with styrene faces a very low free-energy barrier (estimated as 6.0 kcal/mol; note that the B3LYP (+zpe) energy of **7** is lower than that of **6** + styrene), so the transition state must be very early. The prediction of an early, enthalpically barrierless transition state is supported by selectivity observations. For example, cyclopropanation rates with ethyl diazoacetate catalyzed by  $\text{Rh}_2(\text{OAc})_4$  vary by less than a factor of 10 for styrene, 1-hexene, ethyl vinyl ether, and cyclohexene in competition reactions.<sup>2</sup> For perspective, this alkene selectivity is lower than that observed for cyclopropanation with dichlorocarbene.<sup>25</sup> Dichlorocarbene cyclopropanations are themselves thought to be enthalpically barrierless, albeit with a later transition state than **7**.<sup>26</sup>

In contrast, the reaction of **10** is predicted to involve a small but important potential energy barrier (0.5 kcal/mol,<sup>27</sup> including zpe) in its reaction with styrene. The free-energy barrier (estimated as above, plus treating the imaginary frequency as a translational degree of freedom) would be approximately 12 kcal/mol, and variation in this now significant free-energy barrier can allow stereoselectivity and selectivity among alkenes. The transition structure **12** for formation of the minor diastereomer

(24) Lynch, B. J.; Truhlar, D. G. *J. Phys. Chem. A* **2001**, *105*, 2936.

(25) Doering, W. v. E.; Henderson, W. A., Jr. *J. Am. Chem. Soc.* **1958**, *80*, 5274–5277.

(26) Keating, A. E.; Merrigan, S. R.; Singleton, D. A.; Houk, K. N. *J. Am. Chem. Soc.* **1999**, *121*, 3933–38.

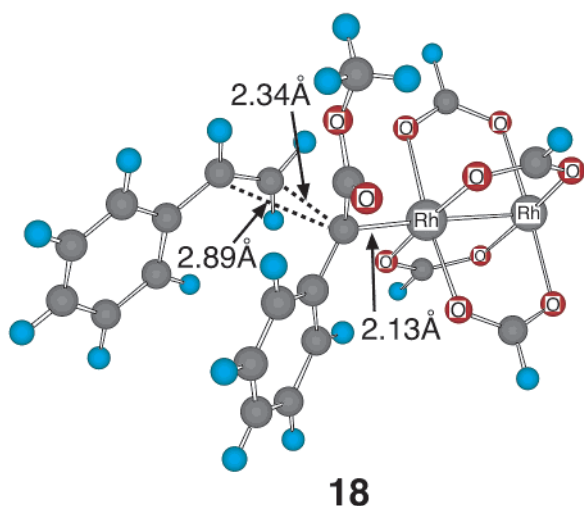
(27) The potential energy barrier is 2.6 kcal/mol (including zpe) versus a weak  $\pi$  complex with a carbene–styrene separation of 3.5 Å. The  $\pi$  complex is kinetically irrelevant because it would not be a bound species on the free energy surface at 25 °C, but its energy is relevant in showing the shape of the potential energy surface.

in this reaction is predicted to be 1.7 kcal/mol higher in energy than **11**. For comparison, reaction of the corresponding phenyl-substituted carbenoid (from  $\text{PhCH}=\text{CHC}(\text{N}_2)\text{CO}_2\text{Me}$ ) with styrene catalyzed by  $\text{Rh}_2(\text{octanoate})_4$  at 25 °C exhibits 50:1 diastereoselectivity (2.3 kcal/mol).<sup>6a,7</sup> The origin of this stereoselectivity will be discussed below.

For comparison, the cyclopropanation of propene with **10** was studied. The best transition structure, depicted in **13**, is predicted to have a barrier 2.0 kcal/mol above the barrier predicted for styrene. This fits well with an experimental relative reactivity of 50 observed for styrene versus 1-hexene in reaction with the corresponding cinnamyl-substituted carbenoid.<sup>28</sup>

In all of the transition structures for cyclopropanations with stabilized carbenoids, the predicted mode of attack of the alkene is best described as “end-on”. One way to gauge this is from the  $\text{Rh}-\text{C}\cdots\text{C}=\text{C}$  dihedral angle, which ranges from 168 to 179° in **11–13** and **18**. The calculations strongly disfavored a side-on approach—an isomer of **13** involving a side-on approach of the propene (see Supporting Information) was disfavored by 4.1 kcal/mol.

**Predicted versus Experimental Isotope Effects.** To predict KIEs for a calculational model as close as possible to the experimental reaction, a limited study of the reaction of styrene with **1** was undertaken. For the cyclopropanation step, three transition structures were located: two for formation of the major diastereomer (differing only in rotational orientation of the ester group) and a third for formation of the minor diastereomer. The lowest energy of these structures, **18**, is closely analogous to **11–13** but with a slightly greater degree of formation of the cyclopropane bonds; the other two structures are shown in the Supporting Information. The predicted preference for the major diastereomer was 1.8 kcal/mol ( $E + \text{zpe}$ )—as found above for the vinyl carbene, this is consistent with experimental selectivities.<sup>6a,7</sup>



On the basis of structure **18**, <sup>13</sup>C KIEs for the reaction of styrene with **1** were predicted from the scaled theoretical vibrational frequencies<sup>29</sup> by the method of Bigeleisen and

(28) Davies, H. M. L.; Panaro, S. A. *Tetrahedron* **2000**, *56*, 4871–4880.

(29) The calculations used the program QUIVER (Saunders, M.; Laidig, K. E.; Wolfsberg, M. *J. Am. Chem. Soc.* **1989**, *111*, 8989–8994) with Becke3LYP frequencies scaled by 0.9614. (Scott, A. P.; Radom, L. *J. Phys. Chem.* **1996**, *100*, 16502–16513).

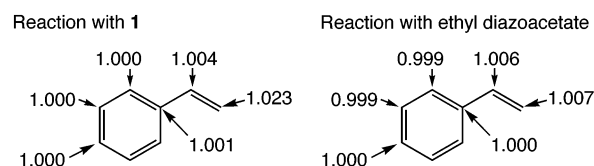


**Figure 4.** Predicted <sup>13</sup>C KIEs ( $k^{12\text{C}}/k^{13\text{C}}$ , 25 °C) for reactions of styrene with **1** (based on transition structure **18**) and with ethyl diazoacetate (based on a 1.5:1 ratio of transition structure **7** and a diastereomeric transition structure leading to the cis product (see Supporting Information)).

Mayer.<sup>30</sup> Tunneling corrections were applied using the one-dimensional infinite parabolic barrier model.<sup>31</sup> The prediction of KIEs for reaction of styrene with ethyl diazoacetate was complicated by the 1.5:1 mixture of trans and cis cyclopropanation products in the reaction. In this case, a weighted average of the isotope effects predicted for **7** and a diastereomeric transition structure leading to the cis product was calculated. The results are summarized in Figure 4.

For the reaction of styrene with **1**, the agreement between predicted and experimental KIEs is striking. In particular, all of the measured KIEs for both the  $\text{Rh}_2(\text{octanoate})_4$ - and  $\text{Rh}_2(\text{-DOSP})_4$ -catalyzed reactions are within the experimental error of the predicted KIEs.<sup>32</sup> Considering the moderate basis set employed theoretically and the differences between the experiment and theoretical model— $\text{Rh}_2(\text{O}_2\text{CH})_4$  versus  $\text{Rh}_2(\text{octanoate})_4$  and  $\text{Rh}_2(\text{-DOSP})_4$ , solution versus gas phase—the agreement between experimental and predicted KIEs is outstanding. This supports the approximate accuracy of **18** as a representation of the solution transition state. By extension, it is likely that **11–13** are also reasonably accurate, and this is supported by excellent predictions of reaction barriers, stereoselectivity, and alkene relative reactivity.

In contrast, the agreement between experimental and predicted isotope effects for the reaction of the unstabilized carbenoid is poor. Considering the caveat given above on the unreliability of structure **7**, the lack of agreement of predictions with experiment is not surprising. One might conclude from this that structure **7** is simply geometrically inaccurate. However, there may also be a problem in the prediction of isotope effects for **7**. Because **7** is not a stationary point on the potential energy surface, the shoehorning of conventional transition-state theory to predict KIEs for **7** is arguably quite suspect. One particular difficulty is that a large part of <sup>13</sup>C KIEs arises, within the Bigeleisen formalism, from a ratio of imaginary frequencies for the reaction coordinate for isotopomers.<sup>30</sup> This contribution to the KIE will not be reliably calculated away from a stationary point by the process employed here.

Since the same level of calculation and basis set was used for both the accurate transition structure **18** and the apparently inaccurate structure **7**, the poor agreement between predicted and experimental KIEs for the unstabilized carbenoid is unlikely to be due to a fundamental problem in the theoretical calculation

(30) (a) Bigeleisen, J.; Mayer, M. G. *J. Chem. Phys.* **1947**, *15*, 261. (b) Wolfsberg, M. *Acc. Chem. Res.* **1972**, *5*, 225. (c) Bigeleisen, J. *J. Chem. Phys.* **1949**, *17*, 675.

(31) Bell, R. P. *The Tunnel Effect in Chemistry*; Chapman & Hall: London, 1980; pp 60–63.

(32) The predicted KIEs in Figure 4 are at 25 °C, while the experimental KIEs with  $\text{Rh}_2(\text{-DOSP})_4$  as catalyst were measured at 0 °C. However, on rounding to thousandths, the predicted KIEs at 0 °C are identical to those in Figure 4. In the isotope effect prediction, most of the <sup>13</sup>C KIE arises from a temperature-independent ratio of imaginary frequencies for the isotopomers. Because of this, there is very little variation in the predicted KIEs with temperature.

itself. For this reason, we still conclude that the basic theoretical predictions for the unstabilized carbenoid, i.e., that cyclopropanation is barrierless and that the transition state is very early, are likely correct. As described above, this qualitative description is consistent both with the KIEs and with other experimental observations.

**Diastereoselectivity in Stabilized versus Unstabilized Carbenoids.** The cyclopropanation of an alkene with a rhodium carbenoid is a highly exothermic bimolecular reaction that would predictably have an early transition state, whether or not the carbenoid is stabilized by conjugation with an aryl or vinyl group. However, stabilization impacts the presence versus absence of an enthalpic barrier for the reaction, and this in turn impacts the position of the transition state and the degree to which it is influenced by steric factors.

When a bimolecular reaction has no potential energy or enthalpic barrier, the rate will still usually be limited by an entropic barrier. The transition state for such reactions occurs when the downward gradient of the enthalpy along the reaction coordinate is equal to the upward gradient of  $-T\Delta S$ .<sup>33</sup> In other words, the variational transition-state dividing surface occurs as soon as the rate of drop in the enthalpy outweighs the narrowing of the dynamic entrance channel. Under the circumstances, the transition state may occur so early that the main enthalpic interaction between molecules is an *attractive* van der Waals interaction. The influence of sterics on selectivity is then limited by two factors. First, any sterically interacting groups must be large enough to have a negative impact when the reacting molecules are still very distant. Second, extremely early transition states are maximally flexible, allowing them to avoid steric interactions. These ideas explain the low diastereoselectivity with unstabilized carbenoids. The transition state is so early and flexible that steric interactions are almost insignificant.

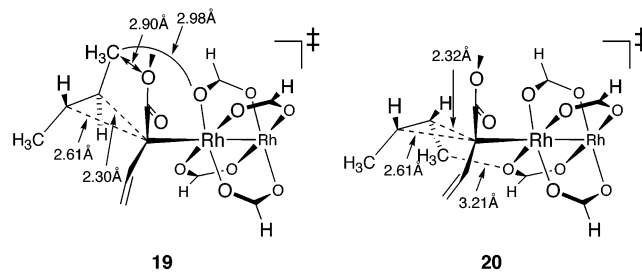
In contrast, the presence of even a small potential energy barrier in a highly exothermic bimolecular reaction is likely to result in a significantly later, less-flexible, transition state. It is enlightening to view the potential energy saddle point in such reactions as the place where the gradient of the favorable (e.g., bonding) interactions starts to outweigh the gradient of the unfavorable (e.g., molecular distortion or steric) interactions. Thus, potential energy barriers generally occur at a stage of the reaction coordinate where repulsive steric interactions have already become significant. Although entropic and other variational transition-state effects will affect the exact position of the transition state, the transition state will normally be near the potential energy saddle point.<sup>34</sup>

Thus, steric interactions can play a substantial role in reactions of stabilized carbenes, precisely because the stabilization results in a potential energy barrier. The particular steric interaction that appears most important arises from the strong preference for the ester group to be twisted out of the plane of the carbenoid carbon. As an alkene approaches either face of the carbenoids, one of the ester's oxygen atoms will invariably be positioned for a steric interaction. In the disfavored transition state **12**, the phenyl group approaches the ester oxygen. The resulting

unfavorable steric interaction is evidenced by a close oxygen–aromatic carbon distance (3.14 Å) and by twisting of the ester and phenyl groups away from each other (by 6 and 4°, respectively). In the favored **11**, the corresponding interaction of the ester oxygen with the  $\alpha$ -hydrogen on styrene involves an oxygen–hydrogen distance of 2.83 Å, and this interaction would be, if anything, attractive.

**Trends in Reactivity and Diastereoselectivity with Stabilized Carbenoids.** An apparent strength of the side-on approach model for cyclopropanations with stabilized carbenoids was that it rationalized in many cases the reactivity of alkenes and structural effects on diastereoselectivity. It was thus important to determine if the calculations here predicting an end-on approach of the alkene could also explain diverse experimental observations. As noted above, the calculations correctly predict several basic trends with good accuracy, including the diastereoselectivity of cyclopropanations of styrene and the reactivity of styrene versus hexene. They also predict well the diastereoselectivity with 1-alkenes. The predicted preference for **11** over the minor diastereomeric transition structure is 2.0 kcal/mol, and the diastereomeric preference with the corresponding phenyl carbene is 1.9 kcal/mol (see Supporting Information for these structures and energies). This may be compared with experimental selectivities ranging from 12:1 to 97:3.<sup>6b,35</sup>

A more complex observation is the nonreactivity of *trans*-disubstituted alkenes in cyclopropanations. This is readily understandable with an end-on approach of the alkene. At the transition state for cyclopropanation of *trans*-2-butene, the methyl group proximal to the rhodium complex cannot avoid steric interactions with both the ester group and an oxygen atom from the tetracarboxylate. With *cis*-2-butene, interaction with the ester is avoided in transition states leading to the favored diastereomer. A slight twist in the angle of attack of the alkene, with an Rh–C···C=C dihedral angle of 170°, minimizes interaction of the methyl group with the tetracarboxylate complex. As a result, *cis*-2-butene's transition structure **20** is strongly favored over the transition structure **19** with *trans*-2-butene, and *trans*-2-butene is predicted to be less reactive by 4.7 kcal/mol.

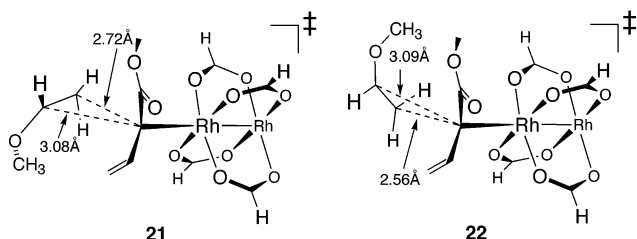


(33) Houk, K. N.; Rondan, N. G. *J. Am. Chem. Soc.* **1984**, *106*, 4293–4294.

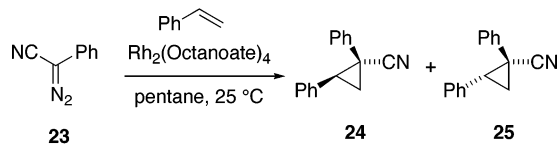
(34) In the particular case of **11**, taking steps of 0.05 Å along the minimum-energy path in both directions afforded geometries with a lower predicted free energy (including entropy and enthalpic and zpe corrections calculated from unscaled frequencies at 298 K). Thus, despite the low potential energy barrier, other effects appear to have relatively little impact on the position of the transition state.

(35) The reaction of the parent vinyl carbenoid with 1-hexene catalyzed by Rh<sub>2</sub>(octanoate)<sub>4</sub> affords mainly the trimer (see ref 3) but gives cyclopropanation adducts in an approximately 12:1 ratio.

catalyzed by  $\text{Rh}_2(\text{octanoate})_4$  affords an 8:1 mixture of diastereomers, less selective than similar reactions with aryl- or alkyl-substituted alkenes.<sup>8b</sup> In the calculational model reaction of methyl vinyl ether with the carbenoid derived from methyl vinyl diazoacetate and  $\text{Rh}_2(\text{O}_2\text{CH})_4$ , the predicted selectivity for transition structure **21** (leading to the major product) over **22** (leading to the minor product) is only 0.9 kcal/mol, in agreement with experimental observations. The predicted barrier for reaction of methyl vinyl ether is 0.8 kcal/mol lower than that for styrene, in excellent agreement with a 4-fold greater reactivity of monosubstituted vinyl ethers over styrene in  $\text{Rh}_2(\text{S-DOSP})_4$ -catalyzed reactions.<sup>28</sup> With the lower barrier, the transition state is much earlier in **21** and **22** than in **11** or **13**, and steric interactions are decreased, resulting in the observed lower stereoselectivity.

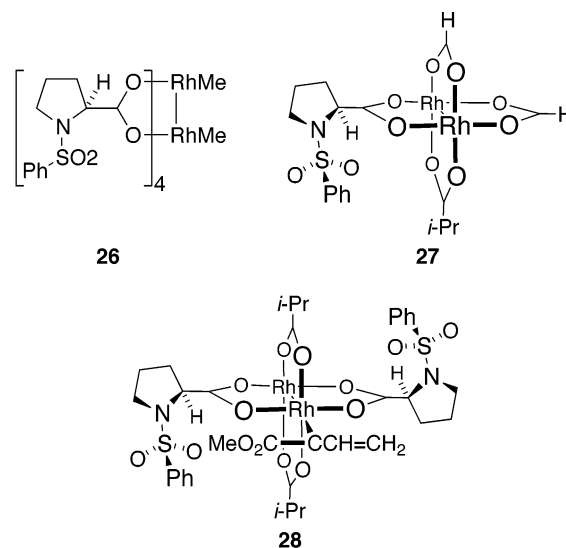


Reactions of nitrile analogues of diazoesters appear to be less diastereoselective. For example, the cyclopropanation of styrene with phenyldiazoacetone nitrile (**23**) catalyzed by  $\text{Rh}_2(\text{octanoate})_4$  affords an 87:13 ratio of **24** and **25**, with the stereochemistry of **24** tentatively assigned as depicted on the basis of the similarity of the NMR spectrum to that of the ester analogue. For the calculational model reaction of the rhodium carbenoid derived from vinyl diazoacetone nitrile with styrene (see Supporting Information), the *cis* arrangement of vinyl and phenyl groups is favored by 0.35 kcal/mol. The decreased stereoselectivity is in keeping with the loss of the steric effect of the ester group discussed above.



**End-On Model for Enantioselective Reactions.** To aid in the development of a model for the understanding and prediction of enantioselectivity in cyclopropanations catalyzed by  $\text{Rh}_2(\text{S-DOSP})_4$ , the low-energy conformations open to the ligands in model complex **26** were studied by molecular dynamics/simulated annealing.<sup>36</sup> Selected ligand conformations were then used in B3LYP optimizations of model **27**. The best of these conformations was then used to study the approach of propene to model carbenoid **28**. Transition structure **29**, leading to the experimentally observed enantiomer, was located in B3LYP calculations using a LANL2DZ basis set on rhodium, 6-31G\* on the carbenoid and olefinic carbons, and a 6-31G basis set on the rest of the lighter atoms. It was assumed in this process

that the DOSP ligands adopt a  $D_2$  symmetric arrangement about the dirhodium core with alternating arylsulfonyl groups oriented toward opposite faces of the complex, as previously discussed.<sup>7</sup> (See Supporting Information for other structures for **27** and **28**.) It should be understood that there are a great many conformations possible for  $\text{Rh}_2(\text{S-DOSP})_4$  and that a much more exhaustive search would be required to adequately explore the conformational space. Nonetheless, our results suggest a tentative model for understanding the origin of the enantioselectivity in these reactions.



Two features of **29** should be noted. First, the phenylsulfonyl groups adopt a propeller-like arrangement that tends to sterically block adjacent quadrants. For **29** as drawn, quadrants I and III (as normally denoted on Cartesian axes) are blocked but the *X*-axis is less sterically encumbered than the *Y*-axis. Second, the carbonyl carbon of the carbomethoxy group is eclipsed with a carboxylate oxygen ( $\text{O-Rh-C-C}$  dihedral angle of  $1^\circ$ ) along the *X*-axis. In **7**, **11–13**, and **18** this dihedral ranges from 12 to  $26^\circ$ , so there is no preference for the carbomethoxy group to be staggered versus the carboxylate oxygens. This is in contrast to previous assumptions.<sup>7,37</sup> (Carbenoids **6** and **10** are nearly eclipsed, while the carbenoid derived from **1** is staggered to minimize steric interactions with the phenyl group. The barrier to rotation about the  $\text{Rh-C}$  bond in **6** is 0.7 kcal/mol.)

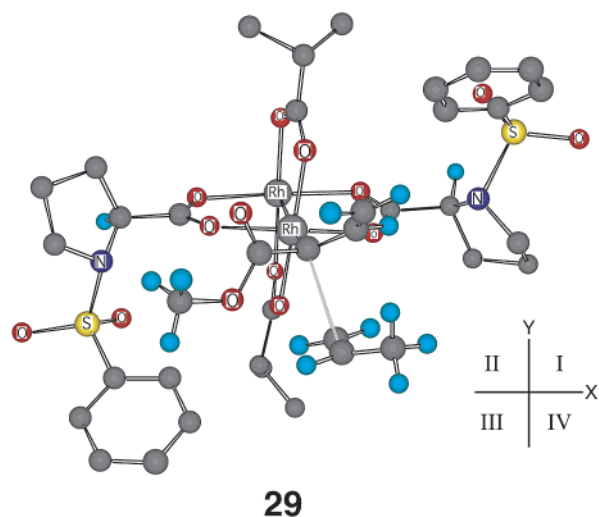
With these factors in mind, a model for understanding enantioselectivity is shown in Figure 5. If the carbomethoxy group is aligned along the less-hindered *X*-axis, then the product is decided by whether the alkene attacks from the top or the bottom. Because the carbenoid carbon is becoming pyramidalized in this attack, the alkene must approach through quadrants I or IV. In Figure 5a, approach of the alkene through quadrant I is hindered, particularly so because the diastereomerically favored approach of the alkene angles an alkyl, aryl, or alkoxy substituent into the center of quadrant I. Quadrant IV is unhindered.

The model of Figure 5 would not apply to reactions catalyzed by  $\text{Rh}_2(\text{S-biTISP})_2$ . Modeling suggests that the  $\text{Rh}_2(\text{S-biTISP})_2$  complex cannot adopt the highly angled propeller arrangement

(36) These studies used default parameters in CS Chem3D Pro, Version 5.0 (1999), CambridgeSoft Corp., Cambridge, MA, treating the carboxylate carbons as alkenyl carbons. Several of the parameters employed were unrealistic—for example the  $\text{Rh-O}$  bond distance was only  $\approx 1.93 \text{ \AA}$ —but were likely satisfactory for the purpose of identifying accessible conformations.

(37) Doyle, M. P.; Winchester, W. R.; Hoorn, J. A. A.; Lynch, V.; Simonsen, S. H.; Ghosh, R. *J. Am. Chem. Soc.* **1993**, *115*, 9968.





29

of arylsulfonyl groups found in **29**, and it is not surprising that  $\text{Rh}_2(\text{S-biTISP})_2$  provides opposite stereochemical results.

On the basis of this analysis, a modified predictive model for  $\text{Rh}_2(\text{S-DOSP})_4$ -catalyzed cyclopropanation is proposed using the end-on approach of the alkene (Figure 6) as a replacement of the original side-on model (Figure 1). The enantiodifferentiation is caused by interaction of the alkene substituents with the blocking aryl component of the arylsulfonyl. The newly modeled alignment of the arylsulfonyl groups in a highly angled propeller arrangement (Figure 5) places these blocking groups in different quadrants from the original model. Thus, in Figure 6, the alkene would be predicted to approach from the front, and this would lead to the observed asymmetric induction.

## Conclusions

The experimental  $^{13}\text{C}$  KIEs are indicative of an early, asynchronous transition state for the cyclopropanation of styrene with rhodium carbenoids, but this is a qualitative interpretation. The KIEs afford only a very vague picture of the transition state, and they would not by themselves exclude alternative mechanisms, including stepwise cyclopropanations and mechanisms not involving discrete rhodium carbenoids at all. However, the combination of isotope effects with theoretical calculations leads to stronger implications.

The close agreement between experimental and theoretically predicted KIEs for the reaction of the **1** with styrene works in two complimentary ways to provide information on the mechanism. First, it shows that transition structure **14** provides a quantitative interpretation of the KIEs. It is certainly possible, in principle, that some alternative mechanism could also lead to the prediction of the experimental isotope effects, but the simplest interpretation of the KIEs is that the actual transition state, in solution and with the real catalyst, looks much like **14**. Second, the agreement of experimental and predicted KIEs provides overall support for the validity and accuracy of the theoretical method. This is very important in studying such a large system, as the choice of theoretical approach and basis set is necessarily limited. The calculated energetics for these reactions are also consistent with the experimental diastereoselectivity and alkene selectivity observed in reactions of aryl- and vinyl diazoacetates, as well as kinetic observations in these reactions and the low reactivity of *trans*-substituted alkenes. Although the prediction of KIEs fails for the difficult barrierless

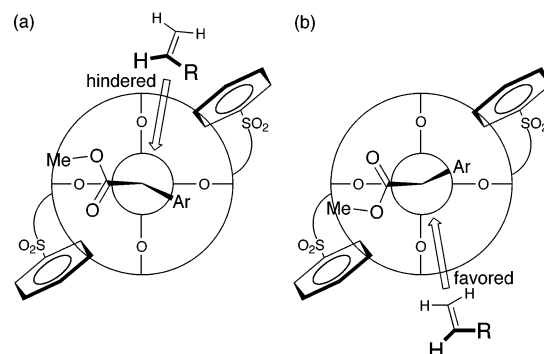


**Figure 5.** Model for understanding enantioselectivity in cyclopropanations catalyzed by  $\text{Rh}_2(\text{S-DOSP})_4$ . (a) Approach of the alkene is hindered by an aryl group. (b) The experimentally preferred enantiomer arises from attack of the alkene from the open quadrant.

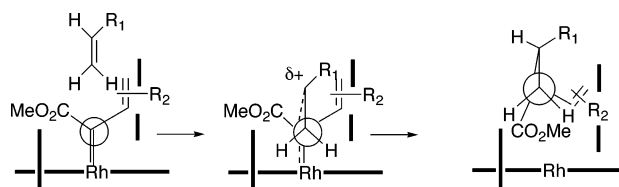


**Figure 6.** “End-on” model for cyclopropanations with stabilized rhodium carbenoids.

reaction of unstabilized carbenes, overall the theoretical calculations fare extremely well.

With some credibility given to the theoretically predicted structures, the origin of selectivity effects in these reactions can be analyzed. In an unstabilized carbenoid, the cyclopropanation transition state is enthalpically barrierless and thus is so early that steric manipulation cannot easily bring about high diastereoselectivity. In stabilized carbenoids, there is an enthalpic barrier and the transition state is late enough for steric interactions to foster diastereoselectivity. In an end-on approach of the alkene to the carbenoid, substituents on the alkene avoid interaction with the carbenoid ester group, accounting for the observed diastereoselectivity in these reactions. Lower diastereoselectivity is observed when this steric interaction is decreased in cyanocarbenoids. In a revised model for asymmetric cyclopropanations catalyzed by  $\text{Rh}_2(\text{S-DOSP})_4$ , the end-on approach of the alkene accounts for the observed enantioselectivity.

These ideas and the detailed transition-state geometries should allow a refined understanding of other enantioselective reactions of rhodium carbenoids as well as the rational design of new cyclopropanation catalysts and reactions. This work is underway.

## Experimental Section

### Cyclopropanation of Styrene with Methyl Phenyl diazoacetate (**1**).

**Example Procedure.** Styrene (10.7 g, 103 mmol) was filtered through 1 mL of silica gel directly into a solution of 80 mg (0.10 mmol) of  $\text{Rh}_2(\text{octanoate})_4$  in 60 mL of dry pentane. To the resulting mixture was added at 25 °C 15.0 g (85.3 mmol) of **1** by syringe pump over 30 min. After the addition was complete, an aliquot was removed and analyzed by  $^1\text{H}$  NMR in  $\text{CDCl}_3$ . The conversion of the styrene was found to be 84% on the basis of the integration of the styrene  $\beta$ -vinylic signals versus product  $-\text{OCH}_3$  groups. The assumed uncertainty in the relative integrations was  $\pm 8\%$ , giving an uncertainty in the conversion of  $\pm 1\%$ .<sup>38</sup> The reaction mixture was directly chromatographed on silica gel 60 (240–400 mesh) with pentane as eluent. Fractions containing styrene were combined and concentrated by distillation at atmospheric

pressure in the presence of  $\approx 5$  mg of butylated hydroxytoluene (BHT), and the residue was distilled at reduced pressure to afford 1.22 g (11.7 mmol) of styrene.

A closely analogous reaction was taken to 83% conversion and afforded 1.50 g of recovered styrene. A similar reaction using 97 mg (0.05 mmol) of  $\text{Rh}_2(\text{S-DOSP})_4$  as catalyst in 50 mL of pentane at 0 °C was taken to 84% conversion and afforded 1.10 g of recovered styrene.

**Cyclopropanation of Styrene with Ethyl Diazoacetate. Example Procedure.** A mixture of 15 mL (13.6 g, 131 mmol) of styrene, 15 mL of  $\text{CH}_2\text{Cl}_2$ , and 20 mg (0.05 mmol) of  $\text{Rh}_2(\text{OAc})_4$  was stirred for 20 min at 25 °C, and 20 mL (21.7 g, 190 mmol) of ethyl diazoacetate was added dropwise over a period of 5 h. During this addition, an additional 2.5 mg of  $\text{Rh}_2(\text{OAc})_4$  was added after 2.5 h and again after 4.5 h. At the end of the addition, an aliquot of the reaction was analyzed directly by  $^1\text{H}$  NMR after diluting with  $\text{CDCl}_3$ , and the conversion, based on integration of the styrene  $\alpha$ -vinylic signal versus product cyclopropane ring signals (at  $\delta$  1.91 and  $\delta$  2.06), was 80%. None of the starting ethyl diazoacetate was detected. The solvent was removed from the reaction mixture at reduced pressure, and the residue was chromatographed on silica gel using hexanes as eluent followed by distillation to afford 1.18 g of recovered styrene contaminated with 1.7% hexanes.

(38) An 8% error from NMR in the ratio of the product to the starting material would correspond to a change from 84:16 (5.25:1) to 85:15 (5.67:1) (5.67/5.25 = 1.08).

Two closely analogous reactions were taken to 81 and 88% conversion, and afforded 822 and 520 mg of styrene, respectively.

**NMR Measurements.** All samples were prepared using a constant 438 mg of styrene in 5 mm NMR tubes filled with  $\text{CDCl}_3$  to a constant height of 5.0 cm. The  $^{13}\text{C}$  spectra were recorded at 100.58 MHz using inverse gated decoupling, 174 s delays between calibrated  $\pi/2$  pulses, and a 5.999 s acquisition time to collect 191 360 points. Integrations were determined numerically using a constant integration region for each peak. A zero-order baseline correction was generally applied, but in no case was a first-order (tilt) correction applied. Six spectra were obtained for each sample of recovered styrene along with corresponding samples of styrene that were not subjected to the reaction conditions. The resulting  $^{13}\text{C}$  integrations for these spectra are given in the Supporting Information. From the  $^{13}\text{C}$  integrations the KIEs and uncertainties were calculated as previously described.<sup>12</sup>

**Acknowledgment.** Financial support of this work by NIH Grant No. GM-45617 and The Robert A. Welch Foundation (D.A.S.) and the National Science Foundation (Grant CHE 0092490, H.M.L.D.) is gratefully acknowledged.

**Supporting Information Available:** Energies and full geometries of all calculated structures and NMR integration results for all reactions. This material is available free of charge via the Internet at <http://pubs.acs.org>.

JA036025Q